

## The influence of phase mask position upon wavefront coded system doublet imaging system

Chiu, Po-Sheng; Vonmetz, Kurt; Canini, Federico; Urbach, H. Paul

**DOI**

[10.1117/12.2530790](https://doi.org/10.1117/12.2530790)

**Publication date**

2019

**Document Version**

Final published version

**Published in**

Proceedings of SPIE

**Citation (APA)**

Chiu, P.-S., Vonmetz, K., Canini, F., & Urbach, H. P. (2019). The influence of phase mask position upon wavefront coded system: doublet imaging system. In C. F. Hahlweg, & J. R. Mulley (Eds.), *Proceedings of SPIE: Novel Optical Systems, Methods, and Applications XXII* (Vol. 11105). Article 111051I SPIE. <https://doi.org/10.1117/12.2530790>

**Important note**

To cite this publication, please use the final published version (if applicable).

Please check the document version above.

**Copyright**

Other than for strictly personal use, it is not permitted to download, forward or distribute the text or part of it, without the consent of the author(s) and/or copyright holder(s), unless the work is under an open content license such as Creative Commons.

**Takedown policy**

Please contact us and provide details if you believe this document breaches copyrights.  
We will remove access to the work immediately and investigate your claim.

# PROCEEDINGS OF SPIE

[SPIEDigitallibrary.org/conference-proceedings-of-spie](https://www.spiedigitallibrary.org/conference-proceedings-of-spie)

## The influence of phase mask position upon wavefront coded system: doublet imaging system

Po-Sheng Chiu, Kurt Vonmetz, Federico Canini, H. Paul Urbach

Po-Sheng Chiu, Kurt Vonmetz, Federico Canini, H. Paul Urbach, "The influence of phase mask position upon wavefront coded system: doublet imaging system," Proc. SPIE 11105, Novel Optical Systems, Methods, and Applications XXII, 111051I (9 September 2019); doi: 10.1117/12.2530790

**SPIE.**

Event: SPIE Optical Engineering + Applications, 2019, San Diego, California, United States

# The influence of phase mask position upon wavefront coded system: doublet imaging system

Po-Sheng Chiu<sup>\*a,b</sup>, Kurt Vonmetz<sup>b</sup>, Federico Canini<sup>b</sup>, H. Paul Urbach<sup>a</sup>

<sup>a</sup>Dept. of Imaging Physics, Delft University of Technology, Lorentzweg 1, 2628 CJ, Delft, the Netherlands; <sup>b</sup>Datalogic IP Tech S.r.l., Via San Vitalino, 13, Calderara di Reno, 40012, BO, Italy

## ABSTRACT

Cubic phase wavefront coding technique is applied to an imaging system with the aim of extending the depth of field (DOF). The design is based on the wavefront coding method proposed by Dowski and Cathey<sup>1</sup>. The method employs a cubic phase mask (CPM) to modify the point spread function (PSF) of the imaging system under incoherent illumination such that the PSF of the system is formed as an isosceles right triangle, which makes the PSF insensitive to defocus. Researchers have found the optimized values of cubic phase coefficient and the exit pupil distance for the given specifications for solving wavefront coded task-based imaging problem<sup>2</sup>. The extended DOF design is usually based on placing a phase mask exactly in the pupil plane of the imaging system. However, this is not always practical because the complex design of the imaging system leads to a limited practical advantage of this kind of arrangement. In this work, the influence of phase mask position upon wavefront coding technique in the doublet imaging system is studied. The main goal is to find the position where to place the CPM in the imaging system, which type of arrangement can effectively improve the modulation transfer function. Finally, we compare two system configurations, front aperture stop and rear aperture stop in designing the doublet wavefront coded system.

**Keywords:** Wavefront coding, cubic phase mask, task-based imaging

## 1. INTRODUCTION

Extended depth of field (DOF) is highly interested in increasing the detection range by means of simpler imaging system. Reducing the aperture of the imaging lens is useful to increase DOF but sacrifices the system resolution. The optical transfer function becomes narrower; hence less amount of light reaches the image plane and the signal-to-noise ratio (SNR) becomes lower. To maintain the SNR, other approaches such as using refractive element<sup>3,4</sup>, diffractive element<sup>5</sup> and birefringence lens<sup>6</sup> were developed.

Refractive element based axicon can provide a larger focal length than the perfect lens in the visible region by changing the curvature of the slanting angle of the axicon<sup>3</sup>. The other refractive based method is to use progressive lenses to increase DOF. In these kinds of lenses, multiple focal lengths are spatially separated and therefore the combination of different focal lengths allows to extend DOF with reduced resolution<sup>4</sup>. A diffractive based method requires a set of non-binary rings on top of the lens pupil. This creates an unbalanced optical path different across the aperture, thus the pupil is divided and the DOF is extended<sup>5</sup>. Alternatively, research also shows that by proper design the two focal lengths with birefringence material, the focusing range can be extended<sup>6</sup>.

Some of the DOF extension methods require expensive optical components, other needs inserting extra optical components into the existing system which increases system complexity. Wavefront coding refers to a technique which modulating the phase or the amplitude of the wavefront in the optical system. This kind of hybrid imaging system combines optics and signal processing, which maintains the simplicity of the system while improving the system performance. Wavefront coding with the cubic phase mask (CPM) has been proposed by Dowski and Cathey<sup>1</sup>. The basic idea of wavefront coding technique is that the point spread function (PSF) of the incoherent imaging system is modified by assigning a phase or an amplitude pattern in the pupil plane. The pattern is added to the wavefront, thus the distribution of the intensity on the focal plane is adapted. Digital filtering is used to retrieve the object because the image formation mechanisms is modified by the new PSF.

The CPM wavefront coding technique attracts our attention because of the following benefits. Firstly, this technique simply

\*p.chiu@tudelft.nl

adds a phase modulation component into the system. This will be suitable to use in the existing system without affecting much of the original design and maintain the system flexibility. Secondly, the wavefront coded optical system is effectively becoming defocus invariant. Research has shown that the wavefront coding technique with CPM can extend much larger DOF than other phase masks such as the quartic phase mask and the logarithmic phase mask<sup>7</sup>. This is a great advantage on improving functionality of the existing system by using CPM.

In this work, the main goal is to find the position of the CPM in the imaging system, which type of the configurations can effectually improve the modulation transfer function (MTF). Firstly, under the desired DOF and the specific target object of the task-based imaging system, we then decide the aperture diameter of the system. This is often decided according to the manufacturing and size limitations of the system, however, we assume that the system aperture size is controlled by the size of the CPM, which means the size of the CPM is smaller than the imaging lens. With the given problem specifications, the cubic phase coefficient can be derived based on the analytical approximation MTF<sup>8</sup>. Secondly, once we have the optimized design parameters of the task-based imaging system, we can simulate the different layouts of the system. The CPM position upon the wavefront coded system usually attached to the imaging components in the pupil plane, however, it does not always work in the optical system. Research has proven that the position of the CPM should be rearranged in order to get better image quality within the same extended range<sup>9</sup>. Therefore, we used optical design software Zemax to simulate the performance (i.e. MTF, PSF) of the wavefront coded system. Finally, based on the performance and the influence of CPM position of different system configurations, we can choose the suitable setting for the hybrid imaging system.

The paper arranged as follow. In section 2, the design procedure of the CPM system is outlined in Figure 1, and the optimization of the cubic phase coefficient for two different scanning range cases are calculated. The comparison between these two cases are given in the following subsection. Section 3 presents the optical simulation result of different CPM imaging configurations. Section 4 discusses about the findings, and section 5 concludes the paper.

## 2. SYSTEM OPTIMIZATION

By image quality definition, there are two cases of interest for the extension of the depth of field: uniform quality imaging and task-based imaging<sup>2</sup>. The uniform quality imaging which means the image quality is the same both in and out of focus, normal photography and camera are this type of imaging systems. The second case task-based imaging systems is applied on the image with a constant amount of usable information. We are interesting about how does wavefront coding technique applies on capturing a constant amount of usable information from the objects as it moves along a desired DOF, therefore, a task-based imaging system is suitable for the needs.

A noiseless, diffraction-limited imaging system with a circular aperture and a cubic phase element at the pupil plane with the incoherent illumination is assumed. MTF of the optical imaging system is defined as the normalized autocorrelation of the pupil function<sup>10</sup>. The exact MTF is given by this definition in Eq. (1)

$$MTF(u, v) = \left| \frac{\iint_{-\infty}^{\infty} \mathcal{P}(\hat{x}+u, \hat{y}+v) \mathcal{P}^*(\hat{x}-u, \hat{y}-v) d\hat{x} d\hat{y}}{\iint_{-\infty}^{\infty} \mathcal{P}(\hat{x}, \hat{y}) \mathcal{P}^*(\hat{x}, \hat{y}) d\hat{x} d\hat{y}} \right|, \quad (1)$$

where  $\mathcal{P}$  is the normalized pupil function,  $\hat{x} = 2x/D$  and  $\hat{y} = 2y/D$  are the normalized Cartesian coordinates of the pupil, and  $f_x, f_y$  and  $u = \lambda d_i f_x/D, v = \lambda d_i f_y/D$  are the spatial frequencies and normalized spatial frequencies in the  $x$  and  $y$  direction, respectively. For the normalized pupil function,  $\mathcal{P}$  is expressed as

$$\mathcal{P}(\hat{x}, \hat{y}) = circ(\hat{x}, \hat{y}) e^{\{ik[\alpha(\hat{x}^3 + \hat{y}^3)] + W_{20}(\hat{x}^2 + \hat{y}^2)\}}, \quad (2)$$

where  $\alpha$  is the cubic phase coefficient and  $W_{20}$  is the defocus parameter, and the circular function is defined as

$$circ(\hat{x}, \hat{y}) = \begin{cases} 1, & \text{if } \hat{x}^2 + \hat{y}^2 \leq 1 \\ 0, & \text{otherwise} \end{cases}. \quad (3)$$

By substituting  $\mathcal{P}$  from equ. (2) into equ. (1), due to the symmetry of the problem, we can analyze the MTF in either of the two orthogonal directions. Here, one of the normalized spatial frequencies has been set to zero ( $v = 0$ ), which means we concentrate on maximizing the value of the MTF along the  $x$  direction. The exact MTF along either one of the two orthogonal directions ( $u$  and  $v$ ) can be expressed as<sup>8</sup>

$$MTF^e(u, 0) = \frac{1}{\pi} \left| \int_{-\sqrt{1-u^2}}^{\sqrt{1-u^2}} \int_{-(\sqrt{1-\hat{y}^2}-u)}^{\sqrt{1-\hat{y}^2}-u} e^{\{ik[(4W_{20}u)\hat{x} + (6\alpha u)\hat{x}^2]\}} d\hat{x} d\hat{y} \right|, \quad (4)$$

where only exist defocus and cubic phase coefficient in the exact MTF, and the amount of cubic phase shift and tilt are assumed to be zero.

## 2.1 Design procedure

For designing the task-based imaging system, the range of object distances (range of  $d_o$ ), focal length of the imaging element ( $f$ ), aperture diameter ( $D$ ), wavelength and the maximum amount detail from the object that we need to capture for the specific tasks (spatial frequency of interest for the object  $S_{fo}$ ) are the typical specifications. We assume the size of the CPM smaller than the lens, hence the phase of the wavefront will be influenced by the size of the CPM rather than the size of the lens. Without knowing the lens diameter in the beginning, we select the suitable plano-convex lens from a wide variety of diameters and focal lengths in the category<sup>11</sup> with the purpose of designing the experiment in the future. Once we have the design specifications, we can optimize the cubic phase coefficient and the distance between the exit pupil and the imaging plane. The system design flow chart for the given problem specifications is shown in Figure 1.

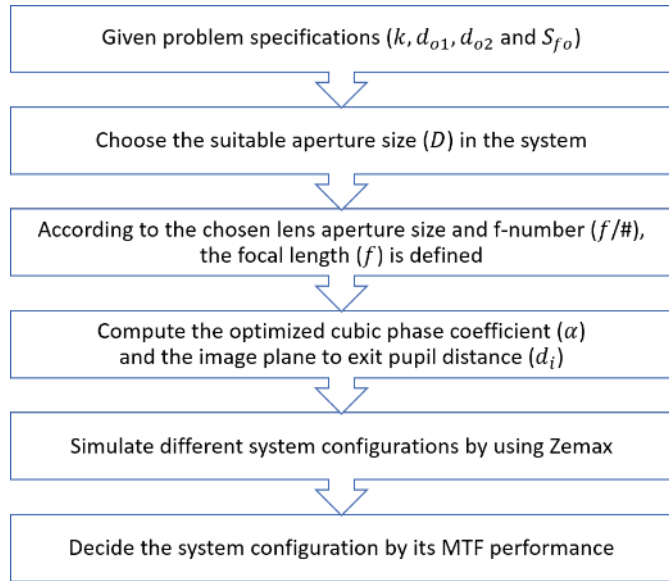


Figure 1. Design flow chart for the task-based imaging system. For the given problem specifications, first to decide the aperture size  $D$  of the system, the aperture size and the f-number  $f/#$  of the imaging lens, then calculate the optimized value of cubic phase coefficient  $\alpha$  and image plane to exit pupil distance  $d_i$ . Once we have the optimized values of  $\alpha$  and  $d_i$ , we use Zemax to simulate different system configurations. Finally, the influence of the CPM position is judged by its MTF performance.

## 2.2 Optimization

The design parameters for cubic phase coefficient  $\alpha$  and image plane to exit pupil distance  $d_i$  that satisfy the optimization criteria. It can be expressed<sup>2</sup> as

$$\max_{\alpha, d_i} \left\{ \min_{d_o, u} \{ MTF^{\alpha 2}(u, 0) \} \right\} \quad \alpha \in \mathcal{R}, d_i \in \mathcal{R}, \\ d_o \in [d_{o1}, d_{o2}], u \in [0, u_{max}(d_o)], \quad (5)$$

where  $d_{o1}$  and  $d_{o2}$  are the required DOF, which are chosen to satisfy the scanning range of the application, and  $u_{max} = 2\pi S_{fo} d_o / kD$  is the normalized spatial frequency of interest in the object plane, where  $D$  is the system aperture diameter and  $k$  is the wavenumber. The maximum normalized spatial frequency of interest  $S_{fo}$  is a function of  $d_o$  and it changes as the object moves along the direction perpendicular to the object plane. Research has shown<sup>12</sup> that to achieve higher tolerance for defocus in the imaging system, it requires the larger cubic phase coefficient, on the other hand, small cubic

phase coefficient has limited effect on extending DOF. For this reason, two different DOF ranges has been chosen to test the feasibility of the optimized system.

The first case is a larger DOF imaging system, and the second case is a comparably small DOF imaging system. The problem specifications are expressed in Table 1, i.e.,  $k$ ,  $d_{o1}$ ,  $d_{o2}$  and  $S_{fo}$ . Wavenumber  $k$  is chosen to be the average value of visible light, and the required DOFs, i.e.  $d_{o1}$  and  $d_{o2}$ , are chosen to satisfy the goal of the system's need. The spatial frequency of interest for the object  $S_{fo}$  is chosen to meet the minimum number of line-pairs in imaging EAN 13 mils barcode, which is the target object for the imaging system.

Table 1. Problem specifications for the task-based imaging problems.

Parameter	Value (case 1)	Value (case 2)	Unit
Wavenumber $k$	$11.4 \times 10^3$		$\text{mm}^{-1}$
Required DOF $d_{o1}$	50	300	mm
Required DOF $d_{o2}$	500	600	mm
Spatial frequency of interest for the object $S_{fo}$	1.5		line-pair/mm
Aperture diameter $D$	5		mm
Lens diameter	6		mm
f-number $f/ \#$	[1, 1.25, 1.5, 1.67, 2, 2.5, 3, 3.33, 3.5, 4, 4.17, 5, 6, 8, 10, 12]		—
Focal length $f$	[6, 7.5, 9, 10.02, 12, 15, 18, 19.98, 21, 24, 15.02, 30, 36, 48, 60, 72]		mm

The diameter of the aperture is chosen to be 5 mm and the imaging lens is 6 mm in diameter. The focal length of the imaging lens affects the distance between the exit pupil and the image plane rather than the cubic phase coefficient. Here, we choose the lens with f-number equals to 8 because of the imaging system requirement. We have the all specifications for designing the task-based imaging system at this moment, one can get the optimized design variables using Equs. (27) and (28)<sup>2</sup>. These optimized values are shown in Table 2.

Table 2. Optimized design parameters for the task-based imaging problems.

Parameter	Value (case 1)	Value (case 2)	Unit
Cubic phase coefficient $\alpha/\lambda$	27.2745	2.6893	—
Image plane to exit pupil $d_i$	[6.4025, 8.1397, 9.9372, 11.1955, 13.7260, 17.7975, 22.1844, 25.2709, 26.9250, 32.0638, 33.9108, 43.7551, 57.8071, 96.5766, 161.6082, 293.2528]	[6.0901, 7.6413, 9.2043, 10.2738, 12.3659, 15.5761, 18.8360, 21.0153, 22.1468, 25.5096, 26.6650, 32.3964, 39.5069, 54.4437, 70.4179, 87.5414]	mm
Max. spatial frequency of interest $u_{max\ 1}$	0.008267	0.0496	—
Max. spatial frequency of interest $u_{max\ 2}$	0.0827	0.0992	—
Defocus range in DOF $W_{20}/\lambda$	-47.985~54.0731	-4.5248~4.9250	—

### 2.3 Comparison between case 1 and case 2

To compare the performance of these two different DOF optimized imaging systems with that of the traditional imaging system ( $\alpha/\lambda = 0$ ), we have plotted the exact MTF under three different defocus conditions for these two different cases. The three different defocus conditions represent the system in near field, in focus and in far field. The exact MTF of case 1 task-based imaging is shown in Figure 2, where the system specifications are based on Table 1. The vertical red dash lines are the maximum spatial frequencies  $u = u_{max}(d_o)$ , i.e. the minimum number of line-pairs needs in imaging EAN-13 barcode in that particular DOF (near field: 0.008267 line-pair/mm, in-focus: 0.0158 line-pair/mm, and far field: 0.0827 line-pair/mm). The minimum MTF of case 1 in the range of interest is 0.09332. For case 2, the exact MTF of traditional imaging system and wavefront coded system is represented in Figure 3. The MTF of the particular DOF (near field: 0.0496 line-pair/mm, in-focus: 0.0671 line-pair/mm, and far field: 0.0992 line-pair/mm) of the wavefront coded system in case 2 is larger than in case 1. It is because the defocus range in DOF in case 1 is 10 times larger than in case 2, nevertheless the DOF of case 2 is smaller than in case 1. It should be noticed that the worst case MTF in case 2 is larger than 0.25, which is higher than the worst case MTF in case 1. Higher MTF in the desired DOF gives the higher possibility to acquire the necessary usable information from the object, thus this is the trade-off between the desired scanning range and the MTF. In order to set threshold of MTF larger than 0.2, we have to sacrifice the scanning range in the system, in consequence, we choose case 2 for designing the task-based imaging system. Then we use Zemax to simulate the performance of case 2 with different object positions in the system.

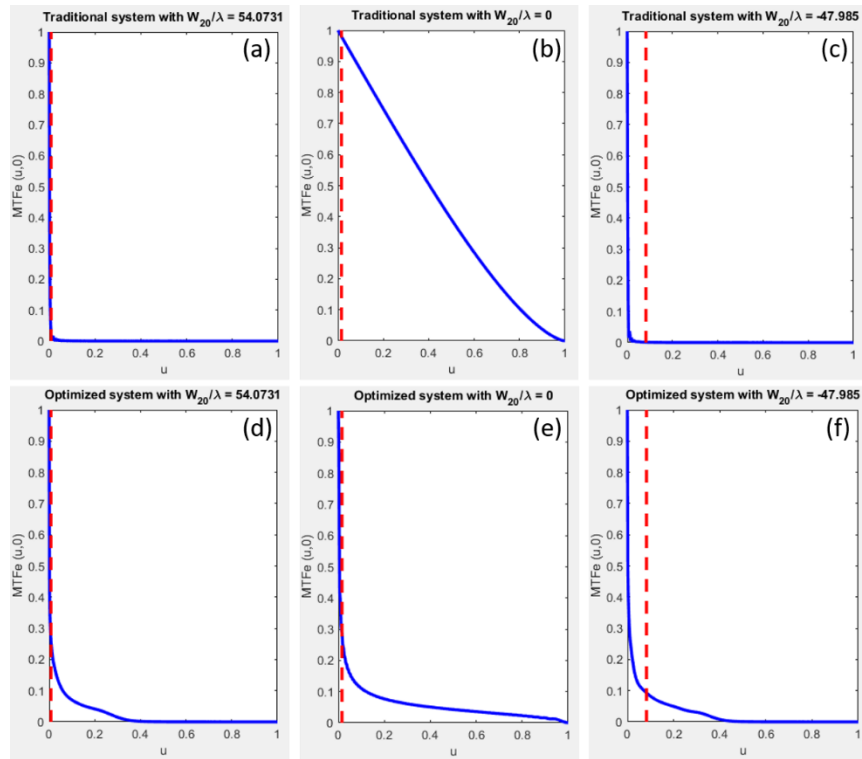


Figure 2. Exact  $MTF(u, 0)$  of traditional imaging system [(a), (b) and (c)] and case 1 wavefront coded task-based imaging system [(d), (e) and (f)]. The red vertical dash line represents the range of spatial frequencies of interest for that particular DOF. (a) Traditional imaging system (near field,  $W_{20}/\lambda \approx 54$  and  $MTF(u, 0) \approx 0.005$ ). (b) Traditional imaging system (in focus,  $W_{20}/\lambda = 0$  and  $MTF(u, 0) \approx 0.980$ ). (c) Traditional imaging system (far field,  $W_{20}/\lambda \approx -48$  and  $MTF(u, 0) \approx 0.001$ ). (d) Optimized imaging system (near field,  $W_{20}/\lambda \approx 54$  and  $MTF(u, 0) \approx 0.246$ ). (e) Optimized imaging system (in focus,  $W_{20}/\lambda = 0$  and  $MTF(u, 0) \approx 0.286$ ). (f) Optimized imaging system (far field,  $W_{20}/\lambda \approx -48$  and  $MTF(u, 0) \approx 0.093$ ).

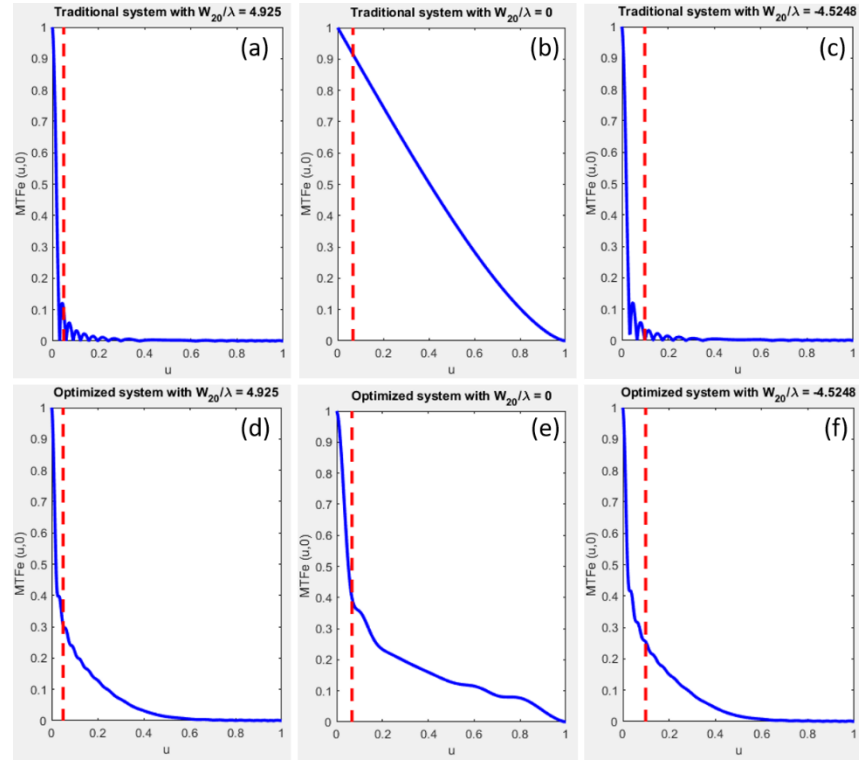


Figure 3. Exact  $MTF(u, 0)$  of traditional imaging system [(a), (b) and (c)] and case 2 wavefront coded task-based imaging system [(d), (e) and (f)]. The red vertical dash line represents the range of spatial frequencies of interest for that particular DOF. (a) Traditional imaging system (near field,  $W_{20}/\lambda \approx 4.93$  and  $MTF(u, 0) \approx 0.092$ ). (b) Traditional imaging system (in focus,  $W_{20}/\lambda = 0$  and  $MTF(u, 0) \approx 0.916$ ). (c) Traditional imaging system (far field,  $W_{20}/\lambda \approx -4.52$  and  $MTF(u, 0) \approx 0.002$ ). (d) Optimized imaging system (near field,  $W_{20}/\lambda \approx 4.93$  and  $MTF(u, 0) \approx 0.304$ ) (e) Optimized imaging system (in focus,  $W_{20}/\lambda = 0$  and  $MTF(u, 0) \approx 0.402$ ) (f) Optimized imaging system (far field,  $W_{20}/\lambda \approx -4.52$  and  $MTF(u, 0) \approx 0.253$ ).

### 3. OPTICAL SIMULATION

In this section, we attempt to consider the influence of the positions of the CPM in hybrid system rather than simply consider the impact of using CPM to extend DOF. The cubic phase coefficient  $\alpha$  has been optimized in section 2. Based on the tradeoff between the MTF and the range of DOF, we choose case 2 as the model. Next, we use Zemax to simulate the MTF performance of different system configurations when placed CPM in the positions of front aperture stop (FAS) and rear aperture stop (RAS). Additionally, we added external defocus according to different object locations (i.e. near field and far filed) to discern the effect on the MTF performance.

#### 3.1 Front aperture stop (FAS)

We design an imaging system with the specifications of plano-convex lens aperture 6 mm, effective focal length 48 mm, the aperture of the CPM 5 mm, and the optimized cubic phase coefficient  $\alpha/\lambda=2.6893$ . We use the following assumptions in the simulation, CPM thickness 5 mm, the CPM material BK7, and the lens thickness 1.6 mm. When the CPM placed before the imaging lens, it is called the front aperture stop because the CPM stays further than the lens to the image plane, and the exit pupil distance is calculated from the CPM to the image plane. We use quick focus in Zemax to find the smallest RMS wavefront plane and it serves as the image plane. From Figure 4 (a), we can see that when there is no CPM in the imaging system, it performs better than the wavefront coded system. It is because the exit pupil distance (-47.7 mm) is approximately equal to the effective focal length (48 mm), hence the MTF performance is better than the wavefront coded system.

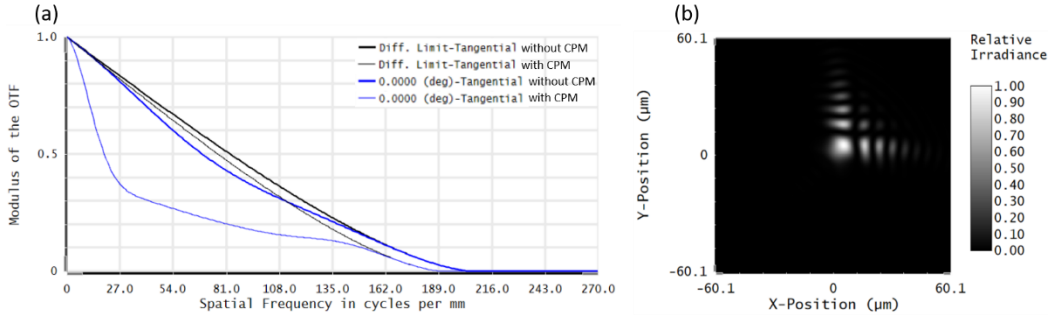


Figure 4. Front aperture stop simulation without external defocus at the object distance 405.6 mm. (a) MTF of the system with CPM and without CPM. (b) PSF of the FAS system without external defocus.

The purpose of using CPM is to increase the tolerance to defocus in the imaging system. Based on the optimized simulation in Section 2, we know that the wavefront coded system can allow certain amount of defocus in the desired scanning range. Therefore, we add external defocus in the wavefront coded system under different object distances to see how the wavefront coding technique improves the MTF in the aberrated system. We assume the thickness of defocus phase plate is 0.5 mm, and it is placed right after the lens. MTF of the FAS system with different defocus and different object distances are shown in Figure 5.

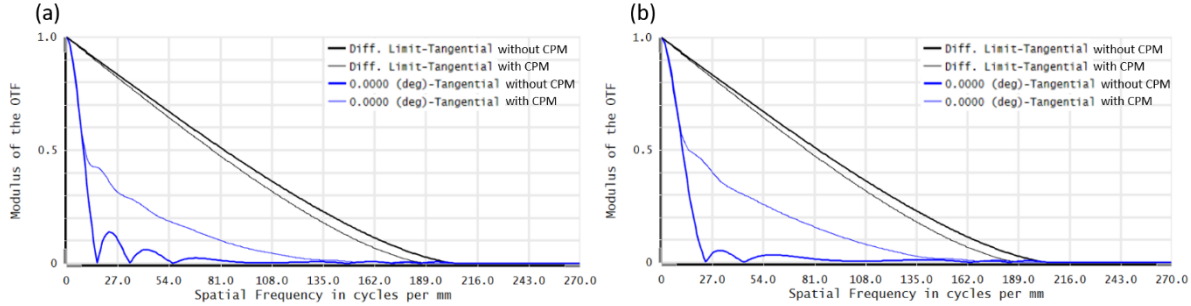


Figure 5. Front aperture stop simulation with external defocus at different object distances. (a) FAS system with external defocus  $W_{20}/\lambda=4.9250$  at the near field, object distance 300 mm. The exit pupil distance is -48.7161 mm, and the entrance pupil distance is 303.2928 mm. (b) FAS system with external defocus  $W_{20}/\lambda=-4.5248$  at the far field, object distance 600 mm. The exit pupil distance is -46.8093 mm, and the entrance pupil distance is 603.2928 mm.

### 3.2 Rear aperture stop (RAS)

When the CPM situated after the imaging lens, it is called front aperture stop because it stays closer than the lens to the image plane. From Figure 6 (a), we can see that when the system with the CPM, it largely improves the MTF of the system. It results from the fact that the exit pupil distance (-43.4 mm) of the system without CPM is approximated 5 mm difference from the focal length, hence the system without CPM is at the out of focus plane.

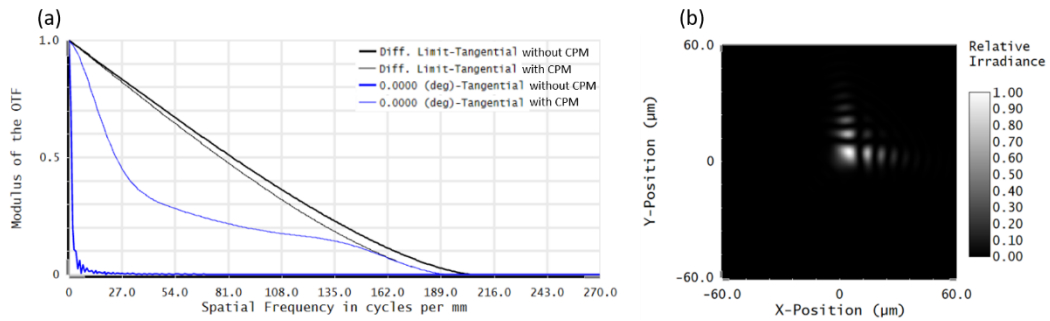


Figure 6. Rear aperture stop simulation without external defocus at the object distance 405.6 mm. (a) MTF of the system with CPM and without CPM. (b) PSF of the RAS system without external defocus.

With the external defocus at different object distances in the system, we can see that the wavefront coded system can effectively improve the MTF. This can be implied from fact that the image plane is out of focus when we remove the CPM. MTF of the RAS system with different external defocus at different object distances are shown in Figure 7.

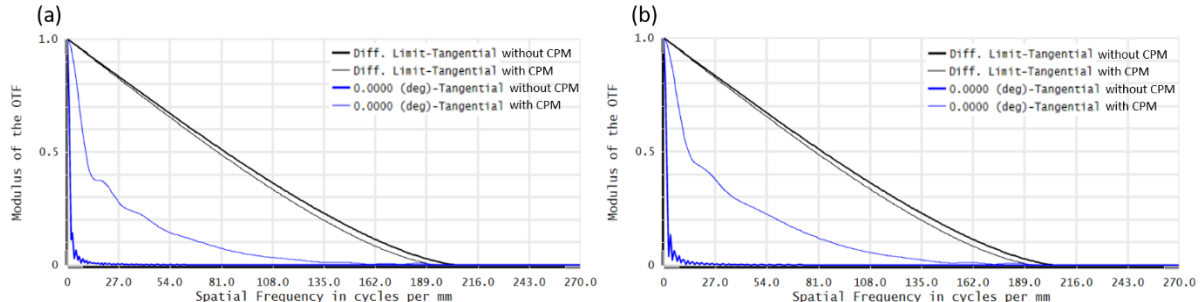


Figure 7. Rear aperture stop simulation with external defocus at different object distances. (a) RAS system with external defocus  $W_{20}/\lambda=4.925$  at the near field, object distance 300 mm. The exit pupil distance is -44.0565 mm, and the entrance pupil distance is 305.1702 mm. (b) RAS system with external defocus  $W_{20}/\lambda=-4.5248$  at the far field, object distance 600 mm. The exit pupil distance is -42.1388 mm, and the entrance pupil distance is 605.1933 mm.

### 3.3 Results

For the same object distance (405.6 mm), there is less than 0.1 difference between the MTF of both wavefront coding configurations. Furthermore, the exit pupil distance in the FAS system is larger than in the RAS system. This is a reasonable result because the CPM is assumed to be smaller than the imaging lens, hence the exit pupil distance is the distance between the image plane and the CPM in the RAS system, this distance is smaller than in the FAS system. Comparing with Figure 5 (a) and Figure 7 (a) or Figure 5 (b) and Figure 7 (b), we can observe that under the same object distance with external defocus ( $W_{20}/\lambda=4.5248$  & 4.5290), the MTF of FAS system is slightly better than the MTF of the RAS system. The reason is that the exit pupil distance of the FAS system is closer to the effective focal length. In addition, the MTF at the far field is performing better than at the near field in both aperture stop systems. Based on the difference of the exit pupil distance between two configurations, we can say that when the CPM placed after the lens in the doublet imaging system, the wavefront coding technique can largely improve the system MTF. However, the exit pupil distance of the FAS system is close to the focal length, hence the result for improving MTF is not as noticeable as in the RAS system.

## 4. DISCUSSIONS

From the optical simulation result in Section 3 we found the difference between the exit pupil distance at the best focus position and the optimized exit pupil distance in Section 2 in both aperture stop configurations. The reasons behind this mismatch are concluded as follows. First, the MTF expression in Reference 2 and 8 are considered only defocus and cubic phase, however, it is never possible to find the lens without other aberrations. The plano-convex lens used in Zemax simulation is aberrated, and the exit pupil distance is influenced by the imperfections of the lens. Second, we assume the aperture of CPM is smaller than the aperture size of the plano-convex lens, hence the CPM is the aperture stop, which determines the amount of light reaching the image plane<sup>13</sup>. The exit pupil distance  $d_i$  in the rear aperture case (CPM placed after the lens) is smaller than in the front aperture case (CPM located before the lens) because the location of the aperture stop. The exit pupil distance depends on the size and the location of the CPM, and this can be illustrated schematically in Figure 8. In the analytical optical solution of the cubic phase wavefront coded system<sup>2</sup>, the position of the CPM and the type (e.g. singlet or compound lens) of the lens are all unknown, which makes the definition of exit pupil location ambiguous. Third, when we calculate the optimized value of the exit pupil distance, it did not take the thickness and the material of the CPM into account. The assumption of the CPM material and the thickness in the optical simulation are BK7 ( $n\approx1.51$ ) and 5 mm, respectively. Thickness and material of the CPM will affect the way of light propagates in the media and the location of the image. Based on the above-mentioned points, we can explain why the exit pupil distance in Zemax simulation is mismatched with the optimized value.

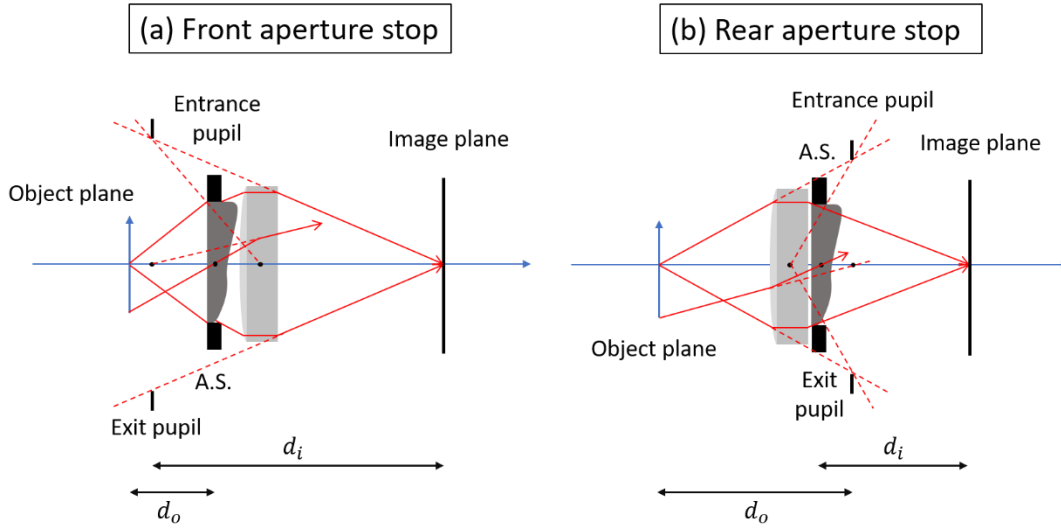


Figure 8. Different positions of the CPM in the wavefront coded system. Dark gray component with holder is the CPM, and the light gray component is the doublet lens. The diameter of the CPM is expected to be smaller than the plano-convex lens, thus the CPM is the aperture stop (A.S.) in the total system. The dimension of the components is exaggerated to show the principle. (a) CPM is placed in front of the lens. (b) CPM at the rear of the lens. When the CPM placed in front of the lens, the exit pupil distance  $d_i$  is larger than in the case of rear aperture stop. This shows that the exit pupil distance depends on the position of the CPM, when the CPM is the A.S. in the imaging system, the exit pupil distance is calculated from the CPM to the image plane.

## 5. CONCLUSIONS

In this work, we compare the MTFs between different configurations of the CPM in the wavefront coded system. Based on the assumption that the diameter of the cubic phase is smaller than the imaging lens, the wavefront coding technique can largely improve the MTF when the CPM placed after the lens (rear aperture stop system) in doublet imaging system. We have pointed out that the location of the CPM is important when designing a wavefront coded system, because the size of the PSF is varying according to the system configurations. For the doublet imaging system, horizontal/vertical size of the PSF of the front aperture stop ( $57 \mu\text{m}$ ) system is larger than in the rear aperture stop system ( $46 \mu\text{m}$ ). Intermediate image from larger isosceles right triangle PSF is more challenge to be restored because it contains more zero points in the PSF. The optimized exit pupil distance considers only defocus and cubic phase coefficient in the derivation<sup>10</sup>, which makes the optimized exit pupil distance differ from the simulation result. Besides, the influences of the material and the thickness in the optical simulation should take into consideration because they will affect the image formation. In general, it is mathematically complicated to incorporate the lens model with considering higher order aberrations and the properties of the CPM into MTF derivations. However, it is necessary to expand the MTF expressions to increase the accuracy of the optimized values and it is one possible direction of future work.

## ACKNOWLEDGEMENT

This research has received funding from the European Union's Horizon 2020 research and innovation program under the Marie Skłodowska-Curie Grant Agreement No. 675745.

## REFERENCES

- [1] Dowski Jr., E. R., and Cathey, W. T., "Extended depth of field through wavefront coding," *Appl. Opt.* 34(11), 1859-1866 (1995).
- [2] Bagheri, S., Silveira, P. E. X., Narayanswamy, R., and de Farias, D. P., "Analytical optical solution of the extension of the depth of field using cubic-phase wavefront coding. Part II. Design and optimization of the cubic phase," *J. Opt. Soc. Am. A* 25(5), 1064-1074 (2008).
- [3] Lit, J. W. Y., and Tremblay, R., "Focal depth of a transmitting axicon," *J. Opt. Soc. Am.* 63(4), 445-449 (1973).
- [4] Sullivan, C. M., and Fowler, C. W., "Progressive addition and variable focus lenses: a review," *Ophthal. Physiol. Opt.* 8(4), 402-414 (1988).
- [5] Chu, K., George, N., and Chi, W., "Extending the depth of field through unbalanced optical path difference," *Appl. Opt.* 47(36), 6895-6903 (2008).
- [6] Sanyal, S., and Ghosh, A., "High focal depth with a quasi-bifocus birefringent lens," *Appl. Opt.* 39(14), 2321-2325 (2000).
- [7] Hu, J., Xu, F., Zhao, X., and Wang, C., "Comparative study of wavefront coding imaging with rotational and non-rotational symmetric phase masks," *Proc. SPIE* 8911, 89110Z (2013).
- [8] Bagheri, S., Silveira, P. E. X., Narayanswamy, R., and de Farias, D. P., "Analytical optical solution of the extension of the depth of field using cubic-phase wavefront coding. Part I. Reduced-complexity approximate representation of the modulation transfer function," *J. Opt. Soc. Am. A* 25(5), 1051-1063 (2008).
- [9] Hsieh, S.-H., Lian, Z.-H., Chang, C.-M., and Tien, C.-H., "The influence of phase mask position upon EDoF system," *Proc. SPIE* 8842, 884207 (2013).
- [10] Goodman, J. W., [Introduction to Fourier Optics], Roberts and Company Publishers, Englewood (2005).
- [11] "<https://www.edmundoptics.com/f/mgfsu2sub-coated-plano-convex-pcx-lenses/13462/>," (6 July 2019).
- [12] Carles, G., Carnicer, A., Bosch, S., "Phase mask selection in wavefront coding systems: A design approach," *Opt. Laser Eng.* 48(7-8), 779-785 (2010).
- [13] Hecht, E., [Optics], Addison Wesley, San Francisco (2002).